



Validation of gamma scanning method for optimizing NaI(Tl) detector model in Monte Carlo simulation

Huynh Dinh Chuong^a, Nguyen Quoc Hung^b, Nguyen Thi My Le^{b,c}, Vo Hoang Nguyen^b,
Tran Thien Thanh^{a,b,*}

^a Nuclear Technique Laboratory, University of Science, VNU-HCM, Viet Nam

^b Department of Nuclear Physics, Faculty of Physics and Engineering Physics, University of Science, VNU-HCM, Viet Nam

^c Faculty of Applied Sciences, Ho Chi Minh City University of Technology and Education, Viet Nam



HIGHLIGHTS

- A model for NaI(Tl) detector was optimized according to the experimental results of the scanning on front and lateral surfaces of the detector with a collimated low-energy photon beams.
- The measured efficiencies with energies between 30 and 1408 keV for point sources at distances of 0 cm and 30 cm from source to detector were determined.
- The simulated efficiencies were calculated using MCNP6 code.
- Good agreement was obtained between measured and simulated efficiencies for the optimized model.

ARTICLE INFO

Keywords:

NaI(Tl) detector
Gamma scanning
Monte Carlo simulation
MCNP6 code
Efficiency calibration

ABSTRACT

The aim of this study is the validation of gamma scanning method for optimizing NaI(Tl) detector model in Monte Carlo simulation. The experimental procedure involved: scanning on front and lateral surfaces of the detector with collimated low-energy photon beam; calibrating the efficiency with energies between 31–1408 keV for point sources at distances of 0 cm and 30 cm from source to the detector. The Monte Carlo code used for the simulations was MCNP6. The diameter and the length of crystal were determined according to the measured results of gamma scanning with a collimated ²⁴¹Am radioactive source. The distance from window to crystal was estimated using transmission measurement recorded on a second detector. The density of reflector was adjusted to obtain the match between measured and simulated values of efficiency ratio of 81 and 31 keV from a ¹³³Ba radioactive source. The optimized model was applied in Monte Carlo simulations to determine the efficiency and energy spectrum response function of NaI(Tl) detector for point source measurements in two configurations. Good agreement was obtained between measured and simulated results.

1. Introduction

Thallium-activated sodium iodide – NaI(Tl) detectors are commonly used for gamma-ray spectroscopy, mainly because of their high detection efficiency, easy maintenance and cost effectiveness. The important features of these detectors are the energy spectrum response function and the efficiency, including full energy peak efficiency (FEPE) and total efficiency (TE). The accurate FEPE calibration curve of NaI(Tl) detectors is required for most of the radioactive monitoring applications (Grujic et al., 2013; Hung et al., 2016; Thanh et al., 2016). The TE calibration curve must be determined for several algorithms of true

coincidence summing correction (Kanisch et al., 2009). Some applications, such as full spectrum analysis (Caciolli et al., 2012) and spectral unfolding algorithm (Baré and Tondeur, 2011), demand also a good database of the energy spectrum response function generated by photon sources. The experimental determination of these features requires the preparation of standard sources, which is quite expensive and time consuming for the laboratories. Especially for in-situ measurements with large samples, such as the monitoring of radioactivity levels in the field, marine environment, waste drum, surface contamination etc., the experimental calibration is very difficult. In such cases, the simulation techniques are more suitable.

* Corresponding author. Department of Nuclear Physics Faculty of Physics and Engineering Physics University of Science, VNU-HCM, 227, Nguyen Van Cu Street, District 5, Ho Chi Minh City, Viet Nam.

E-mail address: tthanh@hcmus.edu.vn (T.T. Thanh).

<https://doi.org/10.1016/j.apradiso.2019.04.009>

Received 19 August 2018; Received in revised form 7 March 2019; Accepted 5 April 2019

Available online 10 April 2019

0969-8043/ © 2019 Elsevier Ltd. All rights reserved.

In recent years, Monte Carlo simulation of NaI(Tl) detectors has been widely applied to determine the efficiency calibration curve and energy spectrum response function for radionuclide quantification in in-situ measurements (Vlastou et al., 2006; Graaf et al., 2011; Baccouche et al., 2012; Grujic et al., 2013; Androulaki et al., 2015, 2016; Zhang et al., 2015; Abdollahnejad et al., 2016; Cinelli et al., 2016; Thanh et al., 2016; Zhukouski et al., 2018). The quantitative results are derived from the simulated efficiencies, thus these values must be accurately evaluated. In order to obtain precise and reliable simulated results, it is necessary to use the exact geometrical parameters of detector for the simulated model. The major parameters of cylindrical NaI(Tl) detectors, which strongly influence the simulated results, include the diameter and the length of crystal, the distance from window to crystal, the thickness and the density of end cap and reflector. Although the manufacturers usually provide the technical specifications of the detector geometry still some details are not completely presented such as the distance from window to crystal, the characteristics of reflector. Besides, in general, the nominal values of the manufacturers can be significantly different from the real values, which affects the accuracy and validity of simulated model. Therefore, the NaI(Tl) detector model should be optimized to obtain good agreement between measured and simulated results, before it is used in Monte Carlo simulation for the applications of radioactive monitoring.

A simple approach to optimize the NaI(Tl) detector model involves experimentally calibrating the FEPE and energy spectrum response function of detector, and then trying to adjust the thickness or density of the reflector by comparing the simulations with the measured results (Saito and Moriuchi, 1981; Tarim et al., 2012; Tam et al., 2016, 2017). However, it is not guaranteed that the optimized model based on this method is the real geometry of detector. Because the simulated results depend on many geometrical parameters, various models may satisfy the match between measured and simulated results for surveyed configuration. In other words, it is only a local solution of a multivariable equation determined by Monte Carlo method. Therefore, we consider that the optimized model obtained by this method is not reliable enough to be applied to configurations that differ from the surveyed configuration.

Another approach involves determining the values of the geometrical parameters by gammagraphy and/or gamma scanning methods and using these values in Monte Carlo simulation. This optimized model is close to real geometry of NaI(Tl) detector, therefore it can be applied in Monte Carlo simulation for all configurations. Gammagraphy is an appropriate method for determining geometrical parameters of the internal structure of NaI(Tl) detectors (Salgado et al., 2012) and high-purity germanium (HPGe) detectors (Boson et al., 2008; Chuong et al., 2016). However, the cost of gammagraphy instruments is quite expensive, so the application of this method is restricted. Gamma scanning method was applied to evaluate the characteristics of NaI(Tl) detectors (Ashrafi et al., 2006) and HPGe detectors (Cabal et al., 2010; Haj-Heidari et al., 2016; Maidana et al., 2016) for developing detector model in Monte Carlo simulation. Gamma scanning systems are constructed with low cost, so this method can be widely used in the laboratories. However, in fact, there have not been many detailed studies about the application of gamma scanning method for NaI(Tl) detectors.

This paper describes and validates a procedure based on gamma scanning method to optimize NaI(Tl) detector model in Monte Carlo simulation. The characteristics of NaI(Tl) detector, such as the diameter and the length of crystal, the distance from window to crystal, the density of reflector, were determined according to the measured results of the scanning on front and lateral surfaces of detector with collimated low-energy photon beams. The defined values of these parameters were used to develop an optimized model for the detector. The Monte Carlo simulations were performed using MCNP6 code. The optimized model was validated by comparing the simulations with the measured results in two configurations.

2. Experiments

2.1. Detectors and radioactive sources description

Two model 802 NaI(Tl) detectors supplied by Canberra Inc., with nominal crystal dimensions of 50.8 mm × 50.8 mm (detector-A) and 76.2 mm × 76.2 mm (detector-B) respectively, were used in this study. In there, detector-A is the main object for the modeling, detector-B is used for gamma scanning measurements. The NaI(Tl) detectors were connected to Osprey™ (Canberra, 2014) which are high-performance, fully-integrated multi-channel analyzer (MCA) tubes base that contain everything needed to support scintillation spectrometry. This one compact unit consists of a high-voltage power supply, preamplifier, and a full-featured digital MCA. It was linked through USB connector to the control and data acquisition system. The acquisitions of gamma-ray spectra were driven by GENIE-2000 software (Genie 2000, 2009). The peak and the overlapping peaks in gamma-ray spectra were processed by COLEGRAM software (Lépy, 2004). To reduce the channel shifting of NaI(Tl) detectors (Moghaddam et al., 2016), the spectrometers were set-up in the room with air conditioner device to achieve stable measurement conditions, approximate temperature of 26 °C and humidity of 45%. Besides, the waiting time of 80 min was prepared before long-time measurements, because the detector will operate in a more stable state.

The gamma standard sources supplied by Eckert & Ziegler Group, including ⁵⁴Mn, ⁶⁰Co, ⁶⁵Zn, ¹⁰⁹Cd, ¹³³Ba, ¹³⁷Cs, ¹⁵²Eu, ²⁴¹Am, were used to provide gamma and X-rays with energies between 31–1408 keV. The information of these sources is presented in Table 1. These sources are disk shaped high strength plastic with diameter of 25.4 mm and thickness of 6.35 mm. The active diameter of source is 5 mm, and the window thickness is 2.77 mm (Eckert & Ziegler catalogue).

Two sets of experiments were performed in this study. First, scanning measurements on frontal and lateral surfaces of detector-A with collimated low-energy photon beams were conducted to determine the exact geometrical parameters of detector. Second, calibration measurements for detector-A were performed in two configurations to obtain the FEPE and energy spectrum response function.

Table 1
Information of the radioactive sources used in this study (Laboratoire National Henri Becquerel, 2018).

Source	Half-life	E (keV)	Photon emission probability (%)	Activity (Bq)
⁵⁴ Mn	312.19 (3) days	834.85	99.9752 (5)	853 (26)
⁶⁰ Co	5.2711 (8) years	1173.23	99.85 (3)	99356 (2981)
		1332.49	99.9826 (6)	
⁶⁵ Zn	244.01 (9) days	1115.54	50.22 (11)	292 (9)
¹⁰⁹ Cd	461.9 (4) days	88.03	3.66 (5)	2780 (83)
¹³³ Ba	10.539 (6) years	30.9731	118.89 *	29178 (875)
		81.00	33.31 (30)	
		356.01	62.05 (19)	
		661.66	84.99 (20)	
¹³⁷ Cs	30.05 (8) years	661.66	84.99 (20)	33892 (1017)
		121.78	28.41 (13)	
¹⁵² Eu	13.522 (16) years	244.70	7.55 (4)	2152216 (64566)
		344.28	26.59 (12)	
		964.08	14.50 (6)	
		1408.01	20.85 (8)	
		59.54	35.92 (17)	
²⁴¹ Am	432.6 (6) years	59.54	35.92 (17)	34076 (1022)

Note: 35.92 (17) = 35.92 ± 0.17 (*): The value of 118.89 is the sum of the photon emission probabilities of XK_α rays (30.6254, 30.9731 keV), K_β₁ rays (34.9873 keV) and K_β₂ (35.908 keV), because their peaks are overlapped in the measured spectra for the NaI(Tl) detectors.

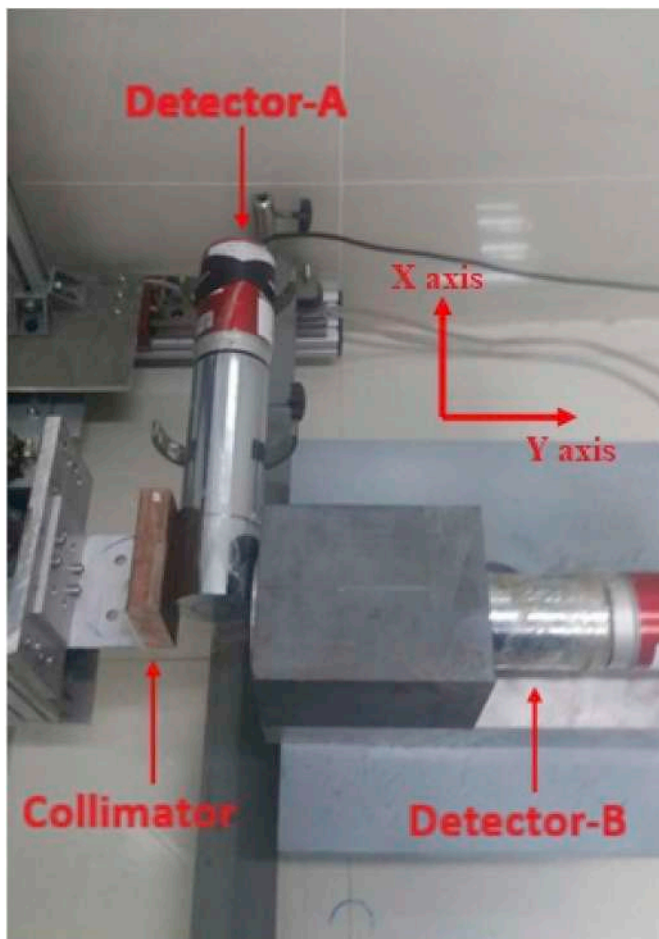


Fig. 1. Experimental set-up of gamma scanning measurements on the lateral surface of detector-A.

2.2. Gamma scanning measurements

A narrow beam of gamma rays emitted from the radioactive sources was generated by using a spot collimator. This collimator was created from a pure copper plate with density of 8.96 g/cm^3 and dimensions of $80 \times 80 \text{ mm}^2$ in surface area, 20 mm in thickness, 3 mm in spot diameter. Besides, a scanning system was constructed to perform the experiments. The stepping motors provided the movement of the collimator along the Ox, Oy, Oz axes so that the gamma beam can irradiate different positions on the surfaces of detector. The definition of Ox, Oy, Oz axes is mentioned in Fig. 1 and Fig. 2. The movement of this scanning system with the uncertainty of 0.01 mm was controlled by software.

For gamma scanning measurements on the front surface of detector-A, it was arranged on the support so that the detector symmetric axis was parallel to the Oy movement axis of the scanning system. First, the collimator was aligned with a laser device to determine the coordinate (x_0, z_0) corresponding to the irradiation of photon beam on the center of the front surface. Then, a ^{241}Am radioactive source was fixed to the collimator entrance, and the collimator end was placed at distance of 1 mm from the detector window. The front surface of detector-A was scanned step by step with a grid spacing of 2 mm on both Ox and Oz directions, covering a square slightly bigger than the diameter of detector end cap. In particular, for the scanning along the central line on Ox direction, the movement increment is 0.2 mm at the locations near the edges of detector. The acquisition program recorded gamma spectra for all locations of the collimator. In addition, similar measurements were performed using a ^{133}Ba radioactive source for some different

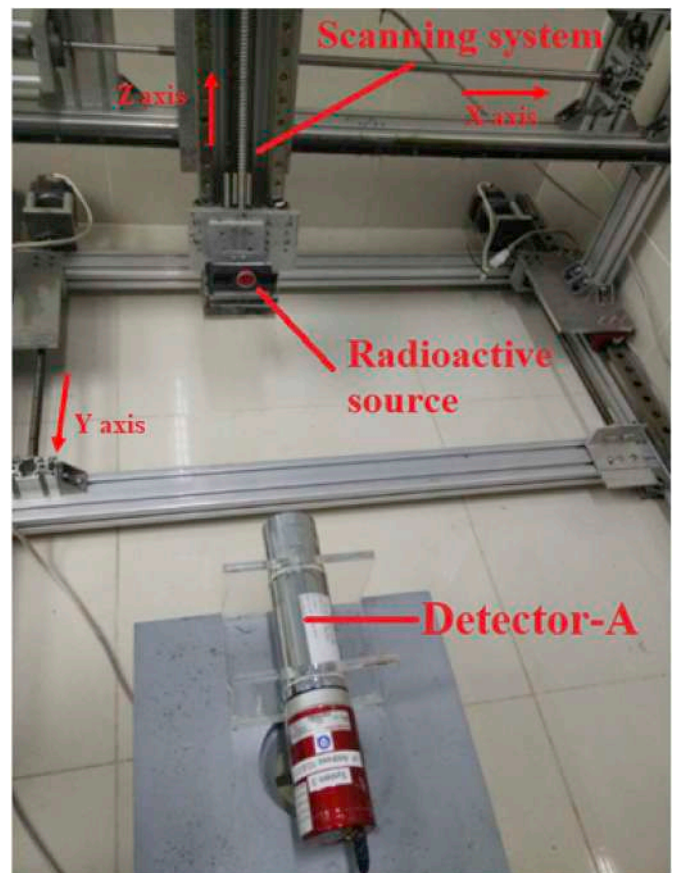


Fig. 2. Experimental set-up of calibrating measurements at distance of 30 cm from source to detector.

locations on the front surface of detector-A.

For gamma scanning measurements on the lateral surface of detector-A, the experimental set-up is shown in Fig. 1. In there, the symmetry axis of detector-A was parallel to the Ox movement axis of the scanning system and perpendicular to the symmetry axis of detector-B. Detector-B is fixed so that its front surface is close to the lateral surface of detector-A and half of its front surface is shielded by detector-A. The collimator end, opposite to front surface of detector-B, was placed at distance of 1.5 mm from the lateral surface of detector-A. The ^{133}Ba and ^{241}Am radioactive sources were used in these measurements. The gamma beam were scanned step by step along the symmetry axis of detector-A with 2 mm increment. In particular, the movement increment is 0.2 mm at the locations near the edges of detector. The acquisition programs recorded gamma spectra of both the detector-A and detector-B for all locations of the collimator.

2.3. Calibrating measurements

The experimental set-up of calibrating measurements is shown in Fig. 2. The detector-A was arranged on a support so that the symmetric axis was parallel to the Oy axis of the scanning system. Radioactive sources were fixed to the scanning system through a plastic sheet. Radioactive sources were moved to locations on the symmetry axis of detector at the distances of 0 cm and 30 cm from the source to detector by the scanning system. Therefore, the measurement configurations were precisely set-up and the influence of scattering events with the surrounding materials was reduced.

For calibrating measurements at distance of 30 cm, the radioactive sources listed in Table 1, including ^{60}Co , ^{133}Ba , ^{137}Cs , ^{152}Eu , ^{241}Am were used. At this distance, the true coincidence summing effects can be ignored. And the monoenergetic radioactive sources which did not

cause true coincidence summing effects, including ^{54}Mn , ^{65}Zn , ^{109}Cd , ^{137}Cs , ^{241}Am were used for calibrating measurements at distance of 0 cm. The measurements were performed to obtain a number of counts in the interesting peaks ranging from 1×10^5 to 3×10^6 . The dead-time for all measurements were less than 5%. The program automatically corrected dead-time losses because the MCA worked in the live-time mode. Besides, the measurement of environmental background radiations also was carried out.

For the data analysis, first, the background spectrum was subtracted from the spectra obtained by the radioactive source measurements. Then, these spectrum data were processed using the COLEGRAM software to obtain the net area under the interesting peaks.

The measured FEPE and relative uncertainty were calculated using the following equations:

$$\epsilon_{\text{Measured}}(E) = \frac{S(E)}{A \times I(E) \times t \times C} \sqrt{a^2 + b^2} \quad (1)$$

$$u_{\text{Measured}} = \sqrt{(u_S)^2 + (u_A)^2 + (u_t)^2 + (u_C)^2} \quad (2)$$

where: S is the net peak area; A is the activity of source (Bq); I is the photon emission probability; t is the acquisition live time (s); C is the correction factor for the radionuclide decay. Besides, u_S , u_A , u_t and u_C are the relative uncertainty of the net peak area, the activity of source, the photon emission probability and correction factors, respectively.

3. Monte Carlo simulation

3.1. Simulated model of NaI(Tl) detector

The vertical cross-section of simulated model for NaI(Tl) detector is shown in Fig. 3. It contains a NaI(Tl) cylindrical crystal, surrounded by a Al_2O_3 reflector and an aluminum end cap, coupled to a photomultiplier (PM) tube on the back. The end cap is separated from the reflector by a very thin air gap. The thickness of this air gap is not shown in the manufacturer's specifications. Besides, the exact modeling of PM tube is very difficult because of its complex structure. Instead, PM tube is treated as an aluminum disk with thickness of 30 mm to account for backscattering (Shi et al., 2002).

Two simulated models of NaI(Tl) detector, including an initial model used the manufacturer's specifications and an optimized model mainly based on the information obtained from the gamma scanning method, were constructed in this study. The values of the geometrical parameters and the density of materials used in these models are shown in Table 2. It can be observed that the major differences between two

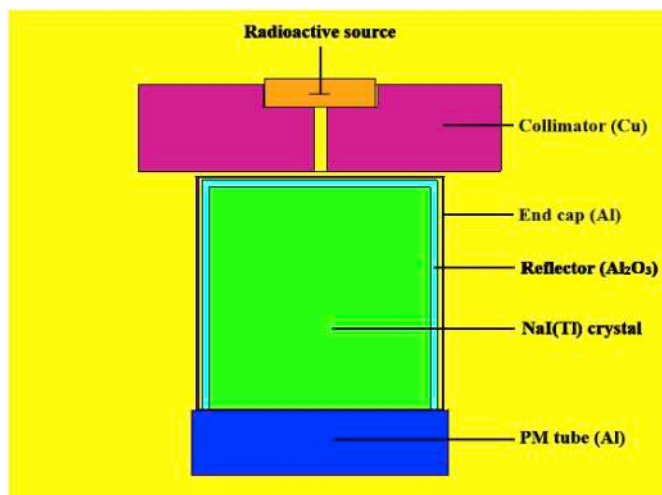


Fig. 3. Vertical cross-section of simulated model for gamma scanning measurement on the front surface of detector-A using MCNP6 code.

models are the distance from window to crystal and the density of reflector. Monte Carlo simulations using MCNP6 code for the same configurations of calibrating measurements were performed with both initial and optimized models.

3.2. Monte Carlo simulation using MCNP6 code

The MCNP6 is a general purpose Monte Carlo radiation transport code developed at the Los Alamos National Laboratory-USA. It is the newest member of the MCNP family of codes, which is one of the most commonly used simulated tools for radiation transport. For users of traditional MCNP, the striking new developments are MCNP6's ability to transport many more particle types at a greatly extended energy range and several significant new capabilities compared to previous versions (Goorley et al., 2016).

In this study, we only consider the interaction of gamma and X-rays with the materials. Therefore, radioactive sources were set to emit only photons, and "Mode P" was used within input files for Monte Carlo simulations. With this condition, the interaction processes of photons such as photoelectric effect, Compton (incoherent) scattering, Thomson (coherent) scattering, pair production and fluorescence emission after photoelectric absorption were simulated during the history of these particles. The transports of electrons generated by the interaction of photons with materials were not tracked. The bremsstrahlung radiations generated from the electrons were simulated according to the "Thick Target Bremsstrahlung" model. The cut-off energy for the photons was set at 1 keV.

The F8 tally, available in MCNP6 code, was used to obtain the deposited energy distribution per incident photon in the crystal volume. When an energy E was deposited into the crystal, a count in the corresponding channel of the spectrum was recorded. In order to achieve an energy spectrum response function consistent with the measured spectra, the channels in the simulated spectra were set based on the energy calibration obtained from the experiments. Thus, the simulated spectra have 2048 channels and the channel energy width is 0.851 keV.

Besides, in measured spectra, peaks are dramatically broadened with a Gaussian shape. This is caused by the fluctuations in the light generation inside the NaI(Tl) crystal, the number of collected charges inside the PM tube and the electronic noise. However, the MCNP6 code does not simulate these physical processes, so the recorded signals do not have any fluctuation. Therefore, it is necessary to consider the energy resolution for simulated spectra by applying a Gaussian function. This technique consists of using the "FT8 GEB" card in MCNP6 code and the experimental full width at half maximum (FWHM) of the Gaussian peak. The experimental FWHM curve as a function of energy was determined by measuring the radioactive sources, listed in Table 1, in the energy range of 60–1408 keV. The FWHM function was defined by the following equation:

$$FWHM(\text{MeV}) = -0.009044 + 0.066599 \times \sqrt{E + 0.071995 \times E^2} \quad (3)$$

where: E is the energy of incident gamma rays (MeV). For the FEPE, the monoenergetic sources were considered to avoid unnecessary interference of peaks in the spectra. The simulated FEPE and relative uncertainty were determined as follows:

$$\epsilon_{\text{Sim}}(E) = \frac{N_p(E)}{N(E)} \quad (4)$$

$$u_{\text{Sim}}(E) = \frac{\sqrt{N_p(E)}}{N_p(E)} \quad (5)$$

where: N_p is the number of records in the full-energy peak, and N is the number of photons emitted by the source in the MCNP6 simulation.

The number of histories was (5×10^8) for the simulations of calibrating measurements and (2×10^9) for the simulations of gamma scanning measurements to keep the relative uncertainty less than 0.5%.

Table 2
Parameters of initial model and optimized model for NaI(Tl) detector.

Parameters of NaI(Tl) detector	Manufacturer's value for initial model	Measured value for optimized model
Diameter of crystal (mm)	50.8	50.7
Length of crystal (mm)	50.8	51.0
Distance from window-crystal (mm)	1.6	2.57
Thickness of reflector (mm)	1.6	1.6
Thickness of air gap (mm)	0.0	0.97
Thickness of end cap (mm)	0.5	0.5
Thickness of PM tube (mm)	30	30
Density of NaI(Tl) crystal (g/cm ³)	3.67	3.67
Density of Al ₂ O ₃ reflector (g/cm ³)	0.55	2.0
Density of air (g/cm ³)	0.001205	0.001205
Density of Al end cap (g/cm ³)	2.699	2.699
Density of Al PM tube (g/cm ³)	2.699	2.699

Table 3
Measured and initial simulated values of FEPE and their uncertainty and relative deviation.

Energy (keV)	Distance of 30 cm			Distance of 0 cm		
	FEPE _{Mea}	FEPE _{Sim}	RD (%)	FEPE _{Mea}	FEPE _{Sim}	RD (%)
30.97	0.001173(38)	0.001357	15.62	–	–	–
59.54	0.001280(39)	0.001377	7.57	0.2562(78)	0.2802	9.36
81.00	0.001411(44)	0.001465	3.79	–	–	–
88.03	–	–	–	0.2827(87)	0.3099	9.63
121.78	0.001437(44)	0.001500	4.42	–	–	–
244.70	0.001253(38)	0.001312	4.73	–	–	–
344.28	0.000981(30)	0.001027	4.65	–	–	–
356.01	0.000971(29)	0.000996	2.49	–	–	–
661.66	0.000494(15)	0.000521	5.55	0.0745(22)	0.0822	10.28
834.84	–	–	–	0.0581(17)	0.0634	9.06
964.08	0.000336(10)	0.000353	5.05	–	–	–
1115.54	–	–	–	0.0429(13)	0.0465	8.28
1173.23	0.000279(8)	0.000290	3.99	–	–	–
1332.49	0.000246(7)	0.000255	3.93	–	–	–
1408.01	0.000230(7)	0.000241	4.85	–	–	–

$$\text{Note.RD}(\%) = \frac{|\text{FEPE}_{\text{Sim}} - \text{FEPE}_{\text{Mea}}|}{\text{FEPE}_{\text{Mea}}} \times 100\%$$

4. Results and discussions

4.1. Evaluation of the initial model

The initial model of NaI(Tl) detector was constructed based on manufacturer's specifications. Table 3 presents measured FEPE and simulated FEPE with the initial model for calibration measurements at distances of 0 cm and 30 cm from source to detector. The simulated FEPE shows a quite high discrepancy from measured FEPE. Specifically, the relative deviations between measured and simulated FEPE are about 8–10% with energies in the range of 60–1115 keV for the measurements at distance of 0 cm, and up to 15% with energy of 31 keV for the measurements at distance of 30 cm. This implies that the reliability of the initial model is not high for the use in Monte Carlo simulation to determine FEPE. Thus, it is necessary to optimize the geometrical parameters of the NaI(Tl) detector.

4.2. Shape and dimensions of crystal

More than 800 gamma spectra were recorded from scanning on front and lateral surfaces of detector-A with a ²⁴¹Am collimated radioactive source. The net peak area corresponding to the energy of 60 keV was determined for each spectrum. These measured results were used to analyze the shape and the dimensions of crystal.

Fig. 4 shows three-dimensional plot of the peak area according to the location of collimator on the Ox and Oz axes for scanning on the front surface. Fig. 5 and Fig. 6 show the plots of the peak area according

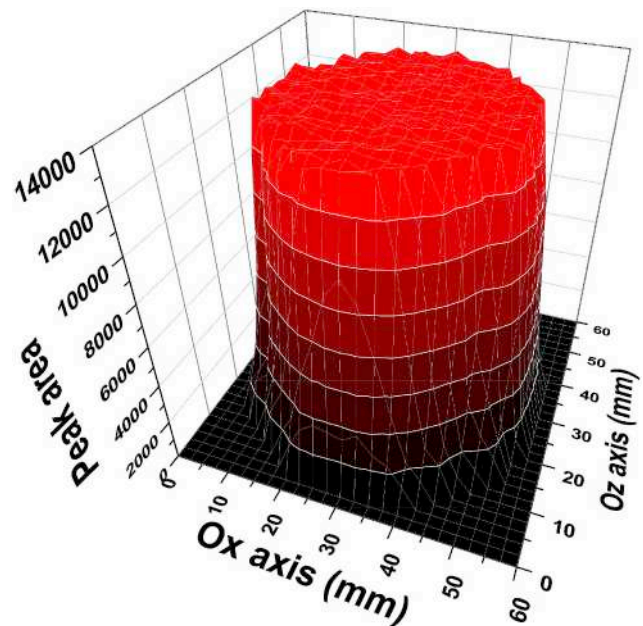


Fig. 4. Three-dimensional plot of the scanning on front surface using a 59.54 keV collimated beam.

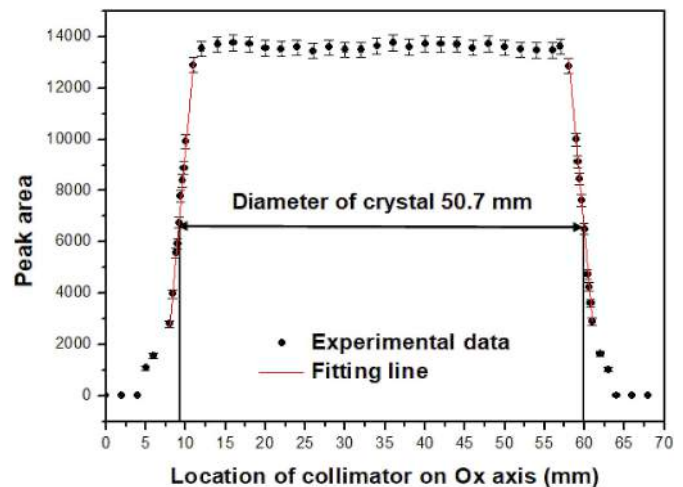


Fig. 5. Plot of the scanning results along the central line of front surface using a 59.54 keV collimated beam.

to the collimator location on the Ox axis for scanning along the central line around front and lateral surfaces, respectively. It can be observed that the peak area does not change significantly with collimator

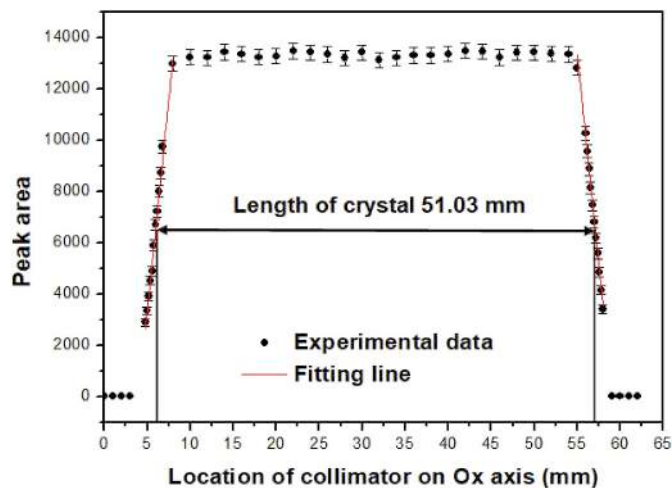


Fig. 6. Plot of the scanning results along the central line of lateral surface using a 59.54 keV collimated beam.

locations in a particular region and rapidly decreases for locations outside of this region. Specifically, for front scanning, the values of the peak area vary from the minimum of 13414 ± 299 to the maximum of 13812 ± 303 , and the average value is 13602 in a circular region. For lateral scanning, the values of the peak area vary from the minimum of 13414 ± 295 to the maximum of 13493 ± 300 , and the average value is 13336 in a range of location from 10 to 54 mm. It is explained that the collimated gamma beam fully irradiates the crystal's active volume with the collimator locations in this region. And the collimated gamma beam does not or partially irradiates the crystal's active volume with collimator locations outside this region. Therefore, the shape and dimensions of the crystal's active volume can be estimated based on the gamma scanning results. From Figs. 4 and 6, it can be concluded that the crystal's active volume has cylindrical shape and the light collection efficiency is uniform for different positions on the surface of crystal.

With the collimator location corresponding to the crystal's edge of detector-A, it can be seen that a half of the collimated beam irradiates the crystal's active volume of detector-A. So, when the contribution of scattering events is ignored, the peak area measured at this location is only a half of the one at location where the collimated gamma beam fully irradiates. Besides, the linear functions can be determined by the least squares fitting for the peak area decrease versus the collimator location in front and lateral scanning, as shown in Figs. 5 and 6. The values of slope, intercept coefficients and its uncertainty are known. Thus, the locations of crystal's edges are estimated by interpolating the value of a half of average peak area in the full irradiation region according to linear functions. And the uncertainty of locations of crystal's edges is calculated by the propagation error formula with the components of the slope, intercept and peak area. The uncertainty of collimator location is not included in these calculations. Because it is small enough (0.01 mm as described in section 2.2) to be ignored. For the front scanning, the locations of left edge and right edge are 9.18 ± 0.03 and 59.86 ± 0.26 , respectively. For the lateral scanning, the locations of top edge and bottom edge are 6.01 ± 0.02 and 57.04 ± 0.24 , respectively. Then, the diameter and the length of crystal are calculated by the subtracting of the locations of crystal's edges. The diameter and the length of crystal are 50.7 ± 0.3 mm and 51.0 ± 0.3 mm, respectively. These results are consistent with the manufacturer's specifications.

4.3. Distance from window to crystal

The gamma-ray spectra were recorded by detector-B for scanning measurements with a ^{133}Ba collimated radioactive source. The net peak area corresponding to the energy of 31 keV was determined for each spectrum. These measured results were used to estimate the location of

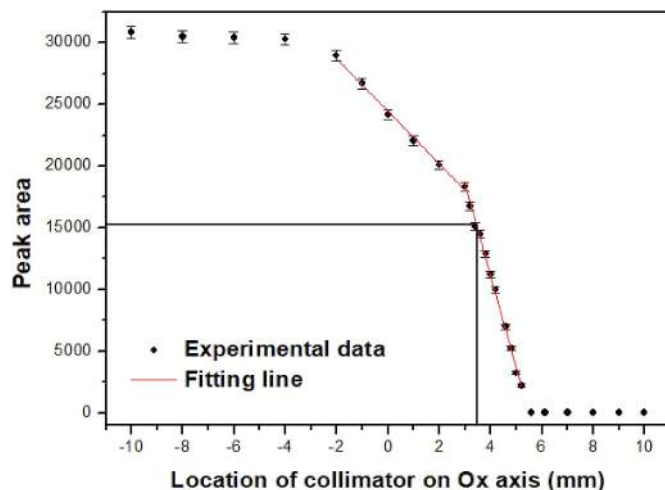


Fig. 7. Plot of the scanning results on detector-B using a 31 keV collimated beam.

detector-A window.

Fig. 7 shows the plot of the peak area according to the location of collimator on the Ox axis for scanning along the central line of detector-B. It can be observed that the peak area does not change significantly with collimator locations in a range of location from -10 to -4 mm. Specifically, the values of the peak area vary from the minimum of 30294 ± 449 to the maximum of 30861 ± 453 , and the average value is 30591 . With these collimator locations, the collimated gamma beam fully irradiates the crystal's active volume of detector-B. Then, the peak area decreases with the increase of the location value in a range of location from -4 to 5.6 mm and is zero in a range of location from 6 to 10 mm. With collimator locations in these ranges, the collimated gamma beam partially irradiates the crystal's active volume of detector-B because it is shielded by detector-A. The energy (31 keV) of X-rays is insufficient to allow it penetrate the thickness of the detector-A.

With the collimator location corresponding to the window of detector-A, it can be seen that a half of the collimated gamma beam irradiates the crystal's active volume of the detector-B. So, when the contribution of scattering events is ignored, the peak area measured at this location is only a half of the one at location where the collimated gamma beam is fully irradiated. Besides, the linear functions can be determined by the least squares fitting for the decrease of peak area according to collimator location, as shown in Fig. 7. Thus, the location of detector-A window is estimated by interpolating the value of a half of average peak area in full irradiation range according to the linear function. The location of detector-A window obtained by this approach is 3.44 ± 0.02 . Then, the distance from window to crystal is 2.57 ± 0.03 mm, which is calculated by the subtracting of the locations of crystal's top edge and the location of window.

4.4. Density of reflector

The reflector acts as a radiation shielding layer between the radioactive source and the crystal. Its effect depends on density, thickness and composition of material. The composition of the reflector for NaI (Tl) detector may be Al_2O_3 or MgO . In previous articles (Tam et al., 2016, 2017), we evaluated the effect of reflector thickness, with the composition of Al_2O_3 and density of 3.67 g/cm^3 (density of the material in the crystal form). However, the reflector material is often in powder form, its density will be smaller in crystal form. Thus, it is necessary to determine the density of the reflector. Actually, it is difficult to simultaneously evaluate many factors such as density, thickness, composition. Therefore, in this work, we selected only to consider the effect of the reflector density.

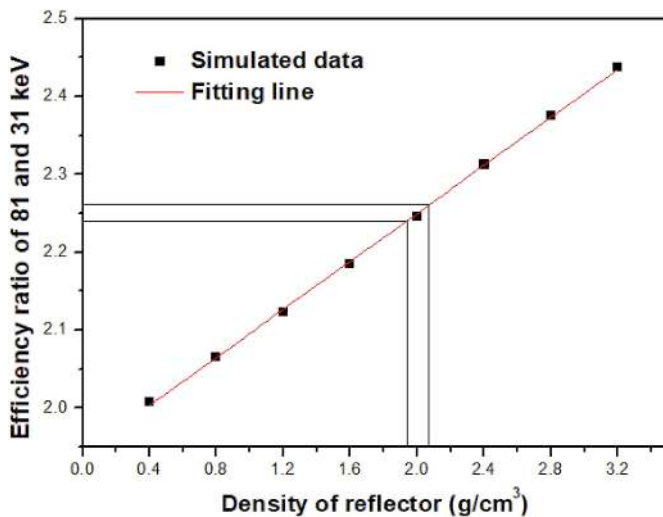


Fig. 8. Linear fitting of the efficiency ratio of 81 and 31 keV versus the density of reflector.

The gamma-ray spectra were recorded at some different positions on front and lateral surfaces of detector-A with a ¹³³Ba collimated radioactive source. The net peak areas corresponding to the energies of 31 and 81 keV were determined for each spectrum. Then, the efficiency ratio of 81 and 31 keV was calculated based on Equation (1). Their values vary from minimum of 2.23 to maximum of 2.26. Besides, a linear relationship between the efficiency ratio of 81 and 31 keV obtained by Monte Carlo simulation and the density of reflector is showed in Fig. 8. The slope and intercept coefficients of linear function were defined by the least squares fitting of simulated data. The density of reflector was estimated by interpolating the measured values of efficiency ratio of 81 and 31 keV according to this linear function.

Fig. 9 shows the density of reflector obtained by this approach at 23 positions on the front and lateral surfaces of detector-A. It can be observed that the density of reflector does not change significantly at surveyed positions. Specifically, their values vary from minimum of 1.89 g/cm³ to maximum of 2.08 g/cm³. Thus, an average value of 2.00 ± 0.08 g/cm³ can be selected to represent the density of reflector.

4.5. Validation of the optimized model

The optimized model of NaI(Tl) detector was constructed based on information obtained from the gamma scanning method. This model

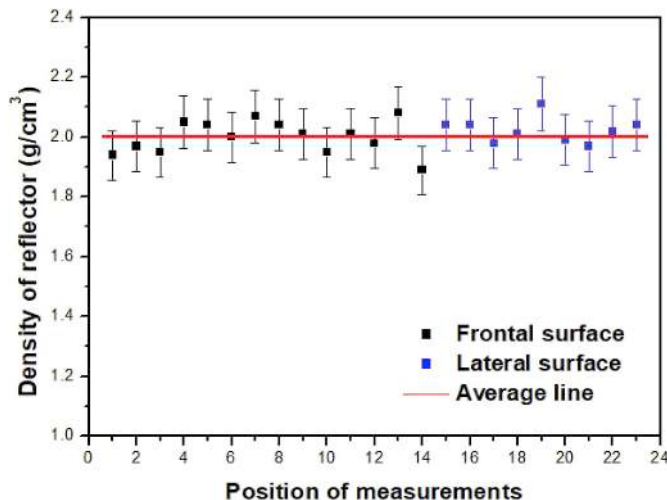


Fig. 9. Density of reflector at some positions on front and lateral surfaces.

Table 4

Measured and optimized simulated values of FEPE and their uncertainty and relative deviation.

Energy (keV)	Distance of 30 cm			Distance of 0 cm		
	FEPE _{Mea}	FEPE _{Sim}	RD (%)	FEPE _{Mea}	FEPE _{Sim}	RD (%)
30.97	0.001173(38)	0.001161	1.05	–	–	–
59.54	0.001280(39)	0.001297	1.34	0.2562(78)	0.2521	1.60
81.00	0.001411(44)	0.001394	1.22	–	–	–
88.03	–	–	–	0.2827(87)	0.2839	0.42
121.78	0.001437(44)	0.001436	0.04	–	–	–
244.70	0.001253(38)	0.001265	1.01	–	–	–
344.28	0.000981(30)	0.000992	1.14	–	–	–
356.01	0.000971(29)	0.000964	0.81	–	–	–
661.66	0.000494(15)	0.000507	2.56	0.0745(22)	0.0771	3.50
834.84	–	–	–	0.0581(17)	0.0596	2.60
964.08	0.000336(10)	0.000343	2.11	–	–	–
1115.54	–	–	–	0.0429(13)	0.0439	2.18
1173.23	0.000279(8)	0.000283	1.35	–	–	–
1332.49	0.000246(7)	0.000249	1.50	–	–	–
1408.01	0.000230(7)	0.000236	2.50	–	–	–

was validated by comparing the simulations with the measured results in calibrating measurements.

Table 4 presents FEPE and simulated FEPE with optimized model for calibrating measurements at distances of 0 cm and 30 cm from source to detector. It can be observed that the relative deviations between measured and simulated FEPE are less than 4% with energies in the range of 31–1408 keV. In most cases, these relative deviations are smaller than the relative uncertainties of the measured FEPE. Besides, these values have decreased significantly compared to those obtained by the simulations with initial model. Furthermore, Fig. 10 also shows the good agreements between measured and simulated gamma spectra of monoenergetic sources including ⁵⁴Mn and ¹³⁷Cs. These results demonstrate that the optimized model of NaI(Tl) detector is precise and reliable for the use in Monte Carlo simulations to determine FEPE and energy spectrum response function.

5. Conclusions

This study revealed that the simulated FEPE using MCNP6 code based on the manufacturer's specifications shows a quite high deviation from measured FEPE. Therefore, it is necessary to find a valid model for a specific NaI(Tl) detector. Here, a procedure for optimizing NaI(Tl) detector model in Monte Carlo simulation was presented. All of important geometrical parameters of NaI(Tl) detector required for the simulated model, such as the diameter and the length of crystal, the distance from window to crystal, the density of reflector, were determined based on the gamma scanning method. This method used a narrow beam of low-energy gamma rays to scan on front and lateral surfaces of detector. The measured values of the diameter and the length of crystal are 50.7 ± 0.3 mm and 51.0 ± 0.3 mm respectively, which corresponded to the manufacturer's specifications. However, the defined values of the distance from window to crystal and the density of reflector, which are 2.57 ± 0.03 mm and 2.00 ± 0.08 g/cm³ respectively, show difference from the manufacturer's specifications. Besides, the uniformity of the light collection efficiency of scintillation crystal also was confirmed. These values were used to build an optimized model for the NaI(Tl) detector in Monte Carlo simulation with MCNP6 code. The optimized model was validated by comparing the simulations with the measured results in two configurations for point source measurements at distances of 0 cm and 30 cm from source to detector. The relative deviations between measured and simulated FEPE are less than 4% with energies in the range of 31–1408 keV. Good agreement was obtained between measured and simulated gamma spectra for some monoenergetic sources. This verifies that the procedure is effective to develop the simulated model for NaI(Tl) detectors.

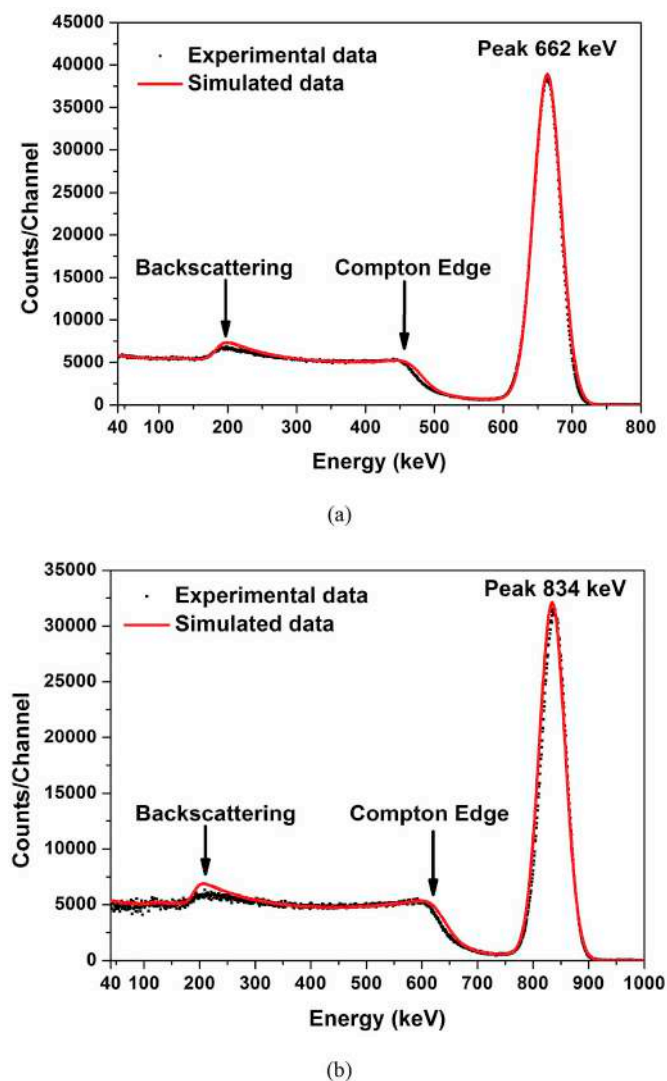


Fig. 10. Comparison between measured spectra and simulated spectra with optimized model of monoenergetic sources, (a) ^{137}Cs , (b) ^{54}Mn .

Acknowledgment

This research is funded by Vietnam National University Ho Chi Minh City (VNU-HCM) under grant number C2018-18-04.

Appendix A. Supplementary data

Supplementary data to this article can be found online at <https://doi.org/10.1016/j.apradiso.2019.04.009>.

References

- Abdollahnejad, H., Vosoughi, N., Zare, M.R., 2016. Design and fabrication of an situ gamma radioactivity measurement system for marine environment and its calibration with Monte Carlo method. *Appl. Radiat. Isot.* 114, 87–91.
- Androulakaki, E.G., Tsabaris, C., Eleftheriou, G., Kokkoris, M., Patiris, D.L., Vlastou, R., 2015. Seabed radioactivity based on in situ measurements and Monte Carlo simulations. *Appl. Radiat. Isot.* 101, 83–92.
- Androulakaki, E.G., Tsabaris, C., Eleftheriou, G., Kokkoris, M., Patiris, D.L., Pappa, F.K., Vlastou, R., 2016. Efficiency calibration for in situ γ -ray measurements on the seabed using Monte Carlo simulations: application in two different marine environments. *J. Environ. Radioact.* 164, 47–59.
- Ashrafi, S., Anvarian, S., Sobhanian, S., 2006. Monte Carlo modeling of a NaI(Tl) scintillator. *J. Radioanal. Nucl. Chem.* 269, 95–98.
- Baccouche, S., Al-Azmi, D., Karunakara, N., Trabelsi, A., 2012. Application of Monte

- Carlo method for the efficiency calibration of CsI and NaI detectors for gamma-ray measurements from terrestrial samples. *Appl. Radiat. Isot.* 70, 227–232.
- Baré, J., Tondeur, F., 2011. Gamma spectrum unfolding for a NaI monitor of radioactivity in aquatic systems: experimental evaluations of the minimal detectable activity. *Appl. Radiat. Isot.* 69, 1121–1124.
- Boson, J., Agren, G., Johansson, L., 2008. A detailed investigation of HPGe detector response for improved Monte Carlo efficiency calculations. *Nucl. Instrum. Methods Phys. Res.* 587, 304–314.
- Cabal, F.P., Lopez-Pino, N., Bernal-Castillo, J.L., Martinez-Palenzuela, Y., Aguilar-Mena, J., Alessandro, K.D., Arbelo, Y., Corrales, Y., Diaz, O., 2010. Monte Carlo based geometrical model for efficiency calculation of an n-type HPGe detector. *Appl. Radiat. Isot.* 68, 2403–2408.
- Cacioli, A., Baldoncini, M., Bezzon, G.P., Broggin, C., Buso, G.P., Callegari, I., Colonna, T., Fiorentini, G., Guastaldi, E., Mantovani, F., Massa, G., Menegazzo, R., Mou, L., Alvarez, C.R., Shyti, M., Zanon, A., Xhixha, G., 2012. A new FSA approach for in situ γ ray spectroscopy. *Sci. Total Environ.* 414, 639–645.
- Canberra, 2014. Osprey™ – Universal Digital MCA Tube Base for Scintillation Spectrometry. http://www.canberra.com/products/radiochemistry_lab/pdf/Osprey-SS-C40303.pdf, Accessed date: 20 June 2018.
- Chuong, H.D., Thanh, T.T., Trang, L.T.N., Nguyen, V.H., Tao, C.V., 2016. Estimating thickness of the inner dead-layer of n-type HPGe detector. *Appl. Radiat. Isot.* 116, 174–177.
- Cinelli, G., Tositti, L., Mostacci, D., Baré, J., 2016. Calibration with MCNP of NaI detector for the determination of natural radioactivity levels in the field. *J. Environ. Radioact.* 155–156, 31–37.
- Eckert & Ziegler, Catalogue of Reference and Calibration Sources. https://www.ezag.com/fileadmin/user_upload/isotopes/isotopes/Isotrak/isotrak-pdf/Product_literature/EZIP/EZIP_catalogue_reference_and_calibration_sources.pdf, Accessed date: 20 June 2018.
- Genie™ 2000 Spectroscopy Software, 2009. Operations. Canberra Industries, Inc.
- Goorley, T., James, M., Booth, T., Brown, F., Bull, J., Cox, L.J., Durkee, J., Elson, J., Fensin, M., Forster, R.A., Hendricks, J., Hughes, H.G., Johns, R., Kiedrowski, B., Martz, R., Mashnik, S., McKinney, G., Pelowitz, D., Prael, R., Sweezy, J., Waters, L., Wilcox, T., Zykaitis, T., 2016. Features of MCNP6. *Ann. Nucl. Energy* 87, 772–783.
- Grujic, S., Đorđević, I., Milosevic, M., Kozmidis-Luburic, U., 2013. Monte Carlo simulation of GM probe and NaI detector efficiency for surface activity measurements. *Radiat. Meas.* 58, 45–51.
- Haj-Heidari, M.T., Safari, M.J., Afarideh, H., Rouhi, H., 2016. Method for developing HPGe detector model in Monte Carlo simulation codes. *Radiat. Meas.* 88, 1–6.
- Hung, N.Q., Chuong, H.D., Vuong, L.Q., Thanh, T.T., Tao, C.V., 2016. Intercomparison NaI(Tl) and HPGe spectrometry to studies of natural radioactivity on geological samples. *J. Environ. Radioact.* 164, 197–201.
- Kanisch, G., Vidmar, T., Sima, O., 2009. Testing the equivalence of several algorithms for calculation of coincidence summing corrections. *Appl. Radiat. Isot.* 67, 1952–1956.
- Laboratoire National Henri Becquerel, http://www.nucleide.org/DDEP_WG/DDEPdata.htm, Accessed date: 20 June 2018.
- Lépy, M.C., 2004. Presentation of the COLEGRAM Software. Note Technique LNHB 04/26.
- Maidana, N.L., Vanin, V.R., Garcia-Alvarez, J.A., Hermida-Lopez, M., Brualla, L., 2016. Experimental HPGe coaxial detector response and efficiency compared to Monte Carlo simulations. *Appl. Radiat. Isot.* 108, 64–74.
- Moghaddam, Y.R., Motavalli, L.R., Hakimabadi, H.M., 2016. Peak shifted properties of the “low background NaI(Tl) detectors”: an experimental study of response function behavior in different temperature and acquisition time. *Radiat. Phys. Chem.* 126, 62–67.
- Saito, K., Moriuchi, S., 1981. Monte Carlo calculation of accurate response functions for a NaI(Tl) detector for gamma rays. *Nucl. Instrum. Methods* 185, 299–308.
- Salgado, C.M., Brandao, L.E.B., Schirru, R., Pereira, C.M.N.A., Conti, C.C., 2012. Validation of a NaI(Tl) detector's model developed with MCNP-X code. *Prog. Nucl. Energy* 59, 19–25.
- Shi, H.X., Chen, B.X., Li, T.Z., Yun, D., 2002. Precise Monte Carlo simulation of gamma ray response functions for an NaI(Tl) detector. *Appl. Radiat. Isot.* 57, 517–524.
- Tam, H.D., Chuong, H.D., Thanh, T.T., Tao, C.V., 2016. A study of the effect of Al_2O_3 reflector on response function of NaI(Tl) detector. *Radiat. Phys. Chem.* 125, 88–93.
- Tam, H.D., Yen, N.T.H., Tran, L.B., Chuong, H.D., Thanh, T.T., 2017. Optimization of the Monte Carlo simulation model of NaI(Tl) detector by Geant4 code. *Appl. Radiat. Isot.* 130, 75–79.
- Tarim, U.A., Ozmutlu, E.N., Gurler, O., Yalcin, S., 2012. The effect of housing material on the NaI(Tl) detector response function. *J. Radioanal. Nucl. Chem.* 293, 425–429.
- Thanh, T.T., Trang, H.T.K., Chuong, H.D., Nguyen, V.H., Tran, L.B., Tam, H.D., Tao, C.V., 2016. A prototype of radioactive waste drum monitor by non-destructive assays using gamma spectrometry. *Appl. Radiat. Isot.* 109, 544–546.
- Van der Graaf, E.R., Limburg, J., Koomans, R.L., Tijs, M., 2011. Monte Carlo based calibration of scintillation detectors for laboratory and in situ gamma ray measurements. *J. Environ. Radioact.* 102, 270–282.
- Vlastou, R., Ntziou, I.Th., Kokkoris, M., Papadopoulos, C.T., Tsabaris, C., 2006. Monte Carlo simulation of γ -ray spectra from natural radionuclides recorded by a NaI detector in the marine environment. *Appl. Radiat. Isot.* 64, 116–123.
- Zhang, Y., Li, C., Liu, D., Zhang, Y., Liu, Y., 2015. Monte Carlo simulation of a NaI(Tl) detector for in situ radioactivity measurements in the marine environment. *Appl. Radiat. Isot.* 98, 44–48.
- Zhukouski, A., Anshakou, O., Kutsen, S., 2018. In situ measurement of radioactive contamination of bottom sediments. *Appl. Radiat. Isot.* 139, 114–120.